

# Constrained Sampling to Guide Universal Manipulation RL

Marc Toussaint<sup>1,2</sup>, Cornelius V. Braun<sup>1</sup>, Eckart Cobo-Briesewitz<sup>1</sup>, Sayantan Audy<sup>1</sup>,  
Armand Jordana<sup>3</sup>, Justin Carpentier<sup>4</sup>

<sup>1</sup>TU Berlin <sup>2</sup>Robotics Institute Germany <sup>3</sup>LAAS-CNRS <sup>4</sup>Inria & DI-ENS, PSL Research University  
Email: toussaint@tu-berlin.de

**Abstract**—We consider how model-based solvers can be leveraged to guide training of a universal policy to control from any feasible start state to any feasible goal in a contact-rich manipulation setting. While Reinforcement Learning (RL) has demonstrated its strength in such settings, it may struggle to sufficiently explore and discover complex manipulation strategies, especially in sparse-reward settings. Our approach is based on the idea of a lower-dimensional manifold of feasible, likely-visited states during such manipulation and to guide RL with a sampler from this manifold. We propose Sample-Guided RL, which uses model-based constraint solvers to efficiently sample feasible configurations (satisfying differentiable collision, contact, and force constraints) and leverage them to guide RL for universal (goal-conditioned) manipulation policies. We study using this data directly to bias state visitation, as well as using black-box optimization of open-loop trajectories between random configurations to impose a state bias and optionally add a behavior cloning loss. In a minimalistic double sphere manipulation setting, Sample-Guided RL discovers complex manipulation strategies and achieves high success rates in reaching any statically stable state. In a more challenging panda arm setting, our approach achieves a significant success rate over a near-zero baseline, and demonstrates a breadth of complex whole-body-contact manipulation strategies.

## I. INTRODUCTION

In the context of Reinforcement Learning (RL), the term universal policy refers to a goal-conditioned policy  $\pi : s, g \mapsto a$  that aims to control from any feasible starting state  $s \in \mathcal{S}$  to any reachable goal  $g \in \mathcal{G}$  [50, 2]. In the field of robotics, universal policies are, in some sense, common and have a long tradition: path finding algorithms are universal and provide a probabilistic completeness guarantee to reach any reachable goal from any start [33]. While the assumptions made in both cases clearly differ, it is interesting to ask more concretely what makes path finding methods effective, while training a universal manipulation policy against a black-box physics simulator seems highly ambitious. In our view, path-finding methods are deeply rooted in computational geometry, providing an understanding of the feasible configuration space given the 3D scene geometry and leveraging this, in particular, to design sampling distributions that guide rapid exploration and provide the foundation for their probabilistic completeness guarantees. In contrast,

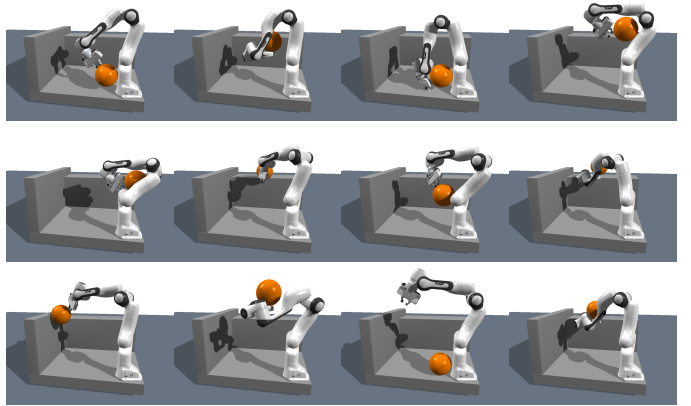


Fig. 1: Random samples from a model-based constrained space that defines the start and goal state distribution of a Constrained Goal-conditional MDP (CG-MDP).

a black-box Markov Decision Process (MDP) formulation of robotic manipulation lacks such structure. In this paper, we propose one avenue to inject such structure into RL by shaping the state visitation distribution using model-based constraints for robotic manipulation, while still treating the dynamics as a black box.

Applying model-based solvers directly to optimize robotic manipulation sequences through contact mode switches is considered challenging, in particular due to the non-linearities and complementarity structure inherent to contact dynamics [49, 3, 10, 56, 20]. In contrast, RL has demonstrated its strength in contact-rich cases [1], arguably due to its implicit smoothing of the underlying control problem [34, 53]. However, RL may struggle to discover manipulation strategies, especially in sparse-reward settings, arguably due to the limits of action-noise-based exploration [44, 59]. A range of approaches have more recently been studied to *combine* the strengths of model-based methods with RL, which we discuss in more detail below. A common approach is to use model-based solvers to generate demonstration trajectories and build on behavior cloning (BC) and imitation learning (IL) paradigms, as well as combinations of BC with RL and offline RL [19, 37, 11].

Our approach is related, but we treat dynamics as a black box and need to fall back on zero-order optimization methods [29] when generating open-loop demonstration trajectories. However, we found that an effective alternative to direct BC from trajectory demonstrations is to guide the *state visitation distribution* of RL using constrained state sampling and, if available, trajectory data. Note that in standard goal-conditional RL formulations [2], the prior distribution  $p_0(s, g)$  over start/goal pairs is assumed given, and drawing samples is considered trivial. This is not the case when dealing with physics: Sampling physically feasible states is a non-convex problem involving collision, contact, and force constraints. Conversely, using such non-trivial samples to guide RL is a powerful approach to integrate first principles.

We first formalize our approach in terms of a novel problem formulation, *Constrained Goal-directed MDPs*, which augments a standard MDP with a model-based differentiable constraint formulation that implicitly defines  $p_0(s, g)$  and thereby provides leverage to guide RL. Using efficient constraint sampling methods and zero-order optimization we can generate both, data of constraint samples, as well as open-loop trajectories between random start/goals. Based on this, our core contribution are various methods to guide RL, using trajectory samples, projected interpolation, scheduling, and optionally BC. We integrate and compare these approaches in our *Sample-Guided RL* framework.

We evaluate our methods first on a minimalistic test scenario: The double sphere (including a sphere object, sphere robot, and basic floor and wall constraints, see Fig. 2). Despite its minimalism, our approach discovers a breadth of complex manipulation strategies in this scenario, and eventually yields a highly reactive universal policy reaching any statically stable configuration from any start state with nearly full success rate. In a second and more advanced scenario, a panda arm manipulates a sphere object with all its links (see Fig. 1). Our approach achieves to train a goal-conditioned policy with significant success rate, compared to a near-zero baseline, and demonstrates a breadth of complex whole-body-contact manipulation strategies.

## II. RELATED WORK

### A. Model-based Manipulation Planning

The literature on model-based robotic manipulation planning reflects a rich understanding of the structure of manipulation in rigid body domains. This includes the exploitation of environmental constraints [39, 51], explicit methods (which explicitly search over contact modes or introduce them as discrete decision variables) [40, 12, 56, 32], and implicit methods (formulations without discrete variables) [49, 41]. However, contact dynamics are inherently stiff and non-smooth and involve complementarities, and therefore pose a fundamentally hard challenge to gradient-based solvers. Pure shooting

methods [29, 51, 54] as well as RL [1] instead treat dynamics as a black-box simulation and avoid these challenges, but they do not exploit the first principles we know about rigid body and contact dynamics. Our approach aims to bridge this gap: While we treat dynamics as black-box, we integrate the aforementioned classical formulations of collision, contact, and force (e.g. friction cone) constraints to define a constrained space of states to guide RL.

### B. RL from Prior Data

A breadth of recent research investigates augmenting RL with data from other sources, including play data [21], expert demonstrations [28], or data from model-based solvers or other policies [37, 19, 7]. In particular, hybrid RL [52] became an established paradigm, where a previously generated static dataset of trajectories is used to guide subsequent online RL phase: Approaches include (i) sequentially performing BC pretraining followed by online RL finetuning [26], (ii) mixing offline and online experience when updating value functions and policies [5, 24], (iii) reward shaping or imitation-style objectives that encourage matching expert state distributions [47, 48], and (iv) replay or reset strategies that bias exploration by initializing episodes from states observed in the offline data [58, 23]. Our approach falls into the last category, but in contrast to prior work, we do not rely on expert demonstrations. Instead, we bias state initialization based on model-based first principles, leveraging our constraint formulation, as well as zero-order trajectory optimization methods.

### C. Goal-conditioned RL & Universal Policies

Universal Manipulation Policies have previously been studied for articulating objects [62], where the notion of *universal* refers to the wide range of objects on which the vision-based policy is applicable. This notion differs somewhat from the concept of universal value functions and goal-conditioned MDPs [50, 2, 18], where the aim is to learn policies that maximize rewards under any task in a fixed MDP (with fixed objects). Our approach falls into the latter category and will train a universal  $Q$ -function and policy to reach any goal state. Several approaches have been proposed to exploit the structure of goal-conditioned RL and improve sample-efficiency, including reward relabeling [2, 4, 25], reward shaping [57], selection or generation of sub- or imaginary goals [43, 46, 8, 9], hierarchical goals [42, 35], intrinsic motivation [38, 36], curriculum-based training [13, 18], and expert guidance [46, 18]. All of these works have in common that they assume that start and goals states can trivially be sampled as part of the problem definition. In contrast, in our setting, we need non-linear constraint solvers to sample from the model-based constraint manifold that defines feasible starts and goals. Further, to our knowledge, none of the existing works has investigated

methods to bias state initialization as the key to guide universal RL.

### III. PROBLEM FORMULATION: CONSTRAINED GOAL-CONDITIONED MDP

We follow the standard definition of a goal-conditioned MDP [50, 2] that we extend with a constraint-based definition of feasible start and goal states. This problem formulation allows us to combine, in a novel way, generic black-box MDP assumptions with first principles on robotic manipulation, force interaction, and feasible states.

We define a constrained goal-conditioned MDP (CG-MDP) by a state space  $\mathcal{S} \subseteq \mathbb{R}^d$ , an action space  $\mathcal{A}$ , dynamics  $p(s'|s, a)$ , a goal-conditioned reward function  $R(s, g)$ , the discount factor  $\gamma \in (0, 1)$ , as well as constraint functions  $g_c, h_c$  which define a set of constrained states

$$\mathcal{S}_c = \{s \in \mathcal{S} : g_c(s) \leq 0, h_c(s) = 0\}, \quad (1)$$

where  $g_c : \mathbb{R}^d \rightarrow \mathbb{R}^{g_c}$  and  $h_c : \mathbb{R}^d \rightarrow \mathbb{R}^{h_c}$  and their Jacobians can be queried point-wise. Given  $\mathcal{S}_c$ , we define the distribution  $p_0(s, g)$  over start and goal states as uniform over  $\mathcal{S}_c$ ,

$$p_0 = \mathcal{U}(\mathcal{S}_c \times \mathcal{S}_c). \quad (2)$$

The problem is then to find a goal-conditioned policy  $\pi : s, g \mapsto a$  to maximize

$$\max_{\pi} \mathbb{E}_{(s, g) \sim p_0} \{V^\pi(s, g)\} \quad (3)$$

$$\text{with } V^\pi(s, g) = \mathbb{E}\{\sum_t \gamma^t R(s_t, g) \mid \pi, s_{t=0} = s\}, \quad (4)$$

with the universal value function  $V^\pi(s, g)$  [50].

First, note that to evaluate the objective (3) and to train a policy, we require a sampler of  $p_0$ . While in standard goal-conditioned MDPs, sampling from  $p_0$  is assumed to be trivial [2], in our case, sampling from  $p_0$  implies solving a non-linear constraint problem, connecting the MDP formulation to standard non-linear programming (NLP) formulations [6].

More importantly, introducing the constraint formulation in CG-MDPs is key to incorporating prior domain knowledge. For instance, in the context of robotic manipulation, we may assume basic collision, contact, and force constraints on states, and start and goal states in particular. The constrained space  $\mathcal{S}_c$  thereby not only implies  $p_0$ , but also provides a prior on what states may be relevant to visit during manipulation that allows us to leverage the power of constraint solvers to guide RL. Note that we do not assume that  $\mathcal{S}_c$  captures *all* states that can be visited by the black-box dynamics  $p(s'|s, a)$ .

#### A. Collision, Contact, and Force Constraints for Robotic Manipulation

We follow existing manipulation planning approaches [49, 10, 56] to formulate constraints in a way that exploits

our structured understanding of the scene in terms of shapes, masses, and forces – a structure that is otherwise hidden in standard MDP formulations. We formulate necessary collision, contact, and force constraints that hold for any state under rigid-body dynamics assumptions, but also add a constraint to impose quasi-static equilibrium (the static Newton-Euler equation). Therefore, in this formulation, start and goal states are constrained to be static, and RL will be guided with a state initialization bias for statically feasible states.

We assume states  $s \in \mathbb{R}^n$  provide generalized coordinates for a scene configuration with  $m$  rigid shapes. For each pair  $(i, j)$ , let  $d_{ij}(s) \in \mathbb{R}$  be the minimal distance between the  $i$ th and  $j$ th shape, and  $n_{ij}(s) \in \mathbb{R}^3$  the corresponding normal.

For all pairs  $(i, j)$ , we impose non-collision constraints. Omitting the dependence on  $s$  for brevity, we have:

$$d_{ij} \geq 0. \quad (5)$$

Further, let  $c_{ij} \in \{0, 1\}$  be a binary contact mode variable. For pairs that are in contact (indicated by  $c_{ij} = 1$ ), we introduce two auxiliary decision variables: the point of attack (POA)  $p_{ij} \in \mathbb{R}^3$  of force interaction between  $i$  and  $j$  [56], and the linear force  $f_{ij} \in \mathbb{R}^3$ . We have point-wise Jacobians for the pair distance  $d_{ij}(s)$ , the normal  $n_{ij}(s)$ , and the distance  $d_{ij}^p(s)$  of the POA  $p_{ij}$  to the surface of shape  $i$  for given generalized coordinates  $s$ . If  $c_{ij} = 1$ , we impose

$$d_{ij} = 0, \quad d_{ij}^p = 0, \quad d_{ji}^p = 0, \quad (6)$$

$$n_{ij}^\top f_{ij} \leq 0, \quad (7)$$

$$\|(\mathbf{I} - n_{ij} n_{ij}^\top) f_{ij}\|^2 \leq \mu^2 \|n_{ij}^\top f_{ij}\|^2, \quad (8)$$

i.e., the shapes touch at  $p_{ij}$  (6), the normal force is positive (7), and the force lies inside a Coulomb friction cone parameterized by  $\mu$  (8).

To describe statically feasible states, we impose quasi-static equilibrium on each unactuated shape via the static Newton-Euler equation:

$$F_i = M_i g_i^{\text{grav}}, \quad (9)$$

where  $F_i$  is the total 6D wrench on shape  $i$  induced by all contact forces,  $M_i \in \mathbb{R}^{6 \times 6}$  is the inertial matrix of  $i$ , and  $g_i^{\text{grav}}$  the gravity vector expressed in the local frame.

## IV. METHODS

### A. Constrained State Sampling

To tackle sampling from the constrained space  $\mathcal{S}_c$  and thereby from  $p_0$ , we aim to leverage an efficient non-linear constrained optimization method and thereby exploit the point-wise differentiability of the constraints  $g_c$  and  $h_c$ . As is the case in manipulation planning through contacts and task-and-motion planning (see Sec. II), our constraint problem is hybrid, including continuous as well as discrete decision variables (the contact mode  $c_{ij}$ ). However, as we only need to sample, we do not have

to find a single optimum and search over all possible contact modes but rather can randomly sample contact modes and address the constraints (5-8) conditional to a fixed  $c_{ij}$ .

Concerning sampling  $c_{ij}$ , in this study we assume a single non-actuated object  $i = 1$  (which is the focus of manipulation) and a finite set of potential support shapes  $S \subseteq \{2, \dots, m\}$ . Randomly imposing support contacts with too many shapes typically leads to an infeasible constraint problem. We therefore limit the potential number of active support contacts to 3, and uniformly first choose between the number 1, 2, or 3 of support contacts, and then uniformly pick the 1-, 2- or 3-tuples of support contacts from  $S$ .

Concerning sampling states  $s$  to fulfill constraints  $g_c(s) \leq 0, h_c(s) = 0$ , we leverage non-convex optimization methods. Concretely, we use an Augmented Lagrangian method [61] to solve the proximal problem

$$\min_s \frac{1}{2} \|s - \bar{s}\|_2^2 \quad \text{s.t. } g_c(s) \leq 0, h_c(s) = 0, \quad (10)$$

where  $\bar{s}$  is a uniform random sample from box constraints, and the non-linear solver is initialized with  $\bar{s}$ . The role of  $\bar{s}$  can be viewed as implying a uniform box prior, which is then projected to the feasible space by solving the proximal problem.

For many random  $c_{ij}$  and  $\bar{s}$ , the resulting NLP might be infeasible or the solver be stuck in a local optimum. To generate a constrained states dataset

$$\mathcal{D}_s = \{s_i\}_{i=1}^S \subset \mathcal{S}_c, \quad (11)$$

we repeat iterating (for random  $c_{ij}$  and box-uniform  $\bar{s}$ ) until  $S$  feasible solutions are found.

Fig. 1 highlights the diversity of configurations this approach generates – and thereby the breadth of the universal policy we aim to train. In our evaluations, Fig. 3(a) reports the total number of constraint evaluations (spent in infeasible and feasible runs) per single feasible state.

### B. Zero-Order Optimization of Open-Loop Trajectories

A powerful approach to guide RL is using model-based trajectory data, e.g. using it for behavior cloning (BC) [37] or combining BC with RL [19]. However, while we have a model-based description of the constrained space  $\mathcal{S}_c$ , our dynamics are black-box, rendering model-based approaches for trajectory generation inapplicable. We instead investigate using zero-order optimization methods and to this end formulate a low-dimensional spline-based open-loop trajectory optimization problem.

Given random start and goal  $(s, g)$ , we aim to find an open-loop control and state trajectory  $u(t), x(t)$  such that  $x(0) = s$  and  $x(T) = g$  under *deterministic* dynamics  $\dot{x} = f(x, u)$ , which are a deterministic version of our underlying MDP. We choose a continuous time control formulation here, as the discrete time step of simulating the dynamics differs from the action time step of the MDP.

We assume  $u(t)$  is B-spline parameterized by  $K$  control points  $\theta_k \in \mathbb{R}^n$ , where  $n$  is the system's control dimension. Given  $(s, g)$ , we solve the optimization problem

$$\min_{\theta} \|\phi(g) - \phi(x(T))\|^2 \quad \text{s.t. } x(0) = s, \dot{x} = f(x, u), \quad (12)$$

where  $\phi(x)$  is a state feature that we design so that a low Euclidean distance  $\|\phi(g) - \phi(x(T))\| \leq \epsilon$  indicates successfully reaching the goal. Note that this formulation does not minimize any control costs. However, our parameterization of controls  $u(t)$  as a B-spline with only a few control points automatically implies smooth trajectories.

We define  $\phi(x)$  as a weighted concatenation of various state features, namely the object position  $p$ , robot generalized coordinates  $q$ , their time derivatives  $\dot{p}, \dot{q}$ , and  $c \in [0, 1]^{m-1}$ . The latter is a continuous indicator for proximity of the object (shape  $i = 1$ ) with all potential supports (shapes  $i = 2, \dots, m$ ). Specifically,  $c_i = 1 - [d_{1i}/\sigma]_{[0,1]}$  where  $[\cdot]_{[0,1]}$  clips the value to the interval  $[0, 1]$ . Therefore,  $c_i = 1$  if the object is in contact with support  $i$ , and decreases linearly to  $c_i = 0$  if support  $i$  has distance  $d_{1i} \geq \sigma$ . To be concrete, in our evaluations, we chose weights  $\phi(x) = (2p, 1q, 0.1\dot{p}, 0.1\dot{q}, 0.1c) \in \mathbb{R}^{6+2n+m-1}$  to design the state feature and thereby optimization objective. Note that the  $c$  component provides the solver with an (implicit) gradient towards reaching the goal contact modes; while components  $p$  and  $\dot{p}$  often have no gradient at all when the initialization has no contact between the robot and the object.

The literature offers a wide spectrum of ideas to solve such a black-box open-loop trajectory optimization problem, including sample-based MPC [29], kinodynamic motion planning [60], or again RL [45]. As it concerns only our secondary problem, it is beyond the scope of the paper to compare these. We instead choose a robust black-box optimization method, namely CMA-ES [22], to solve (12). To generate a trajectory dataset

$$\mathcal{D}_u = \{(s_i, g_i, u_i(t), x_i(t))\}_{i=1}^U, \quad (13)$$

we uniformly sample  $s, g \sim \mathcal{D}_s$ , run CMA-ES, and if feasible add  $(s, g, u(t), x(t))$  to the generated trajectory dataset until  $U$  feasible trajectories (with terminal cost  $\leq \epsilon$ ) are found.

### C. Behavior Cloning from Trajectory Data

Our problem (3) is a standard goal-conditional RL problem for which we can leverage any baseline method by defining observations to encode both, the state  $s$  and goal  $g$ . Rewards  $R(s, g) \in \{0, 1\}$  indicate the object distance to the goal is below a threshold  $\epsilon$ . As our evaluations confirm, the approach of directly sampling random starts and goals  $(s, g) \sim p_0$  during training will lead to ineffective RL. In particular, the likelihood of observing rewards is initially low, leading to a slow or fully muted learning progress.

A well-established approach to guide RL is to integrate behavior cloning (BC): We follow the TD3+BC approach [15], but within the more recent TD7 framework [17], which adds a simple regularization to the policy update objective

$$\max_{\pi} \mathbb{E}_{s,g,a \sim \mathcal{D}} \{ Q(s,g, \pi(s,g)) + \lambda(\pi(s,g) - a)^2 \} , \quad (14)$$

where we include goal-conditioning,  $\mathcal{D}$  is a batch of BC data (see below), and we chose the  $\lambda$  to weigh the BC regularization.

To provide technical detail: To realize behavior cloning based on our trajectory dataset  $\mathcal{D}_u$ , we need to compile continuous-time control B-splines  $u(t)$  to become compatible with the MDP definition. Note that we use 2nd-order B-splines, which are piecewise 2nd-order polynomials. We ensured that the knots between pieces align with the time step discretization of the MDP and that a 2nd-order polynomial piece can be translated uniquely to an action  $a$  (the 20Hz actions are essentially relative position control in joint space; but encoded as single-control-point B-splines, see details in Sec. V-A). By running over  $i = 1, \dots, U$  and  $t = 1, \dots, T$ , the trajectory data can therefore be compiled to a BC dataset

$$\mathcal{D}_{\text{BC}} = \{(s_j, g_j, a_j)\}_{j=0}^{U \cdot T} , \quad (15)$$

with  $g_j = g_i$ ,  $s_j = x_i(t)$  and  $a(u_i(t))$ , with guarantee that these sequences of actions reproduce the exact same state trajectory in a deterministic simulator (such as MuJoCo [55]).

Note, however, that mixing a BC loss to the RL updates in (14) is only possible when for each episode we sample  $(s, g)$  from the available trajectory data. The latter, sampling the start state  $s$  from the available trajectories, is in itself a very strong bias to guide RL. This bears the question whether BC is effective because of the BC loss, or because we bias state initialization along the available trajectory data. In fact, during our research, we gradually shifted from a focus on BC to a focus on biasing state initialization, which turned out crucial and is discussed next.

#### D. Sample-Guided Universal RL

The state visitation distribution in RL can effectively be controlled by adapting the start and goal state distribution  $p_0(x)$  of an episode (the “reset” method) and the time limit (we terminate episodes at the goal, but truncate when a time limit is reached) [14]. The smaller the time limit, the closer we stay to the prescribed  $p_0(x)$ .

As discussed in the context of BC, we can bias state initialization using the available trajectory data. However, in the following, we will also propose an approach based directly on the state data  $\mathcal{D}_s$  without the need for trajectory data  $\mathcal{D}_u$ . Specifically, we propose four strategies to sample start/goals  $(s, g)$  during RL training, including scheduled approaches:

---

#### Algorithm 1 Sample-Guided RL

---

```

1: Generate constrained state data  $\mathcal{D}_s$  solving (10)
2: Generate trajectory data  $\mathcal{D}_u$  solving (12)
3: Compile  $\mathcal{D}_u$  to BC data  $\mathcal{D}_{\text{BC}}$ 
4: Initialize TD7 (nets  $E(s,g)$ ,  $Q(E(s,g),a)$ ,  $\pi(E(s,g))$ )
5: Initialize  $t = 0$ ;
6: while  $t < T_{\text{end}}$  do
7:    $\psi \leftarrow (t + T_{\text{block}})/T_{\text{sched}}$ , clip  $\psi$  in  $[0, 1]$ 
8:   Sample start/goal batch  $B$  using options (16)-(21)
9:   if  $t = 0$ : reset env. with  $(s, g) \sim B$ 
10:  for  $k = 1..T_{\text{block}}$  do
11:     $t \leftarrow t + 1$ 
12:    sample  $a = \pi(s) + \xi$  with clipped  $\xi \sim \mathcal{N}(0, \sigma)$ 
13:    step environment, update replay buffer
14:    gradient update  $E(\cdot), Q(\cdot), \pi(\cdot)$ , opt. with BC
15:    if necessary, reset env. with  $(s, g) \sim B$ 

```

---

1) *Using trajectories, no schedule*: Given  $\mathcal{D}_u$ , we sample

$$i \sim \mathcal{U}\{1, \dots, U\}, \quad t \sim \mathcal{U}[0, T], \quad g = g_i, \quad s = x_i(t) , \quad (16)$$

analogous to the BC dataset.

2) *Using trajectories, scheduled*: Given  $\mathcal{D}_u$  and a training phase variable  $\alpha \in [0, 1]$ , we sample as in (16), except for

$$t \sim \mathcal{U}[(1 - \alpha)T, T] , \quad (17)$$

where we sample at the end interval of the demonstrated trajectories. Here,  $\alpha \in [0, 1]$  is scheduled linearly from 0.1 to 1 during RL training. In addition, in scheduled approaches we adapt the MDP time limit proportional to  $\alpha$ , namely as  $2\alpha T$  to allow for a slack relative to the demonstrated trajectory.

3) *Using nearest state interpolation, no schedule*: Given  $\mathcal{D}_s$ , we sample

$$a, g \sim \mathcal{U}\mathcal{D}_s, \quad t \sim \mathcal{U}[0, 1] , \quad (18)$$

$$s = \underset{s' \in \mathcal{D}_s}{\text{argmin}} \|\phi(s') - \phi((1 - t)a + tg)\| , \quad (19)$$

where  $a, g$  are random constrained states,  $(1 - t)a + tg$  a random the convex interpolation,  $\phi(\cdot)$  a state feature vector embedding (defined in Sec. IV-B), and  $s$  assigned to the feasible state in  $\mathcal{D}_s$  nearest in feature space to the interpolation.

4) *Using nearest state interpolation, scheduled*: Given  $\mathcal{D}_s$ , we sample as in (18), except for

$$t \sim \mathcal{U}[1 - \alpha, 1] , \quad (20)$$

which leads to start states nearer to goal states in early phases of RL.

5) *Baseline: direct sampling*: Given  $\mathcal{D}_s$ , we sample

$$s, g \sim \mathcal{U}\mathcal{D}_s , \quad (21)$$

which aligns with the original problem (3), where  $\mathcal{D}_s$  represents  $p_0$ .

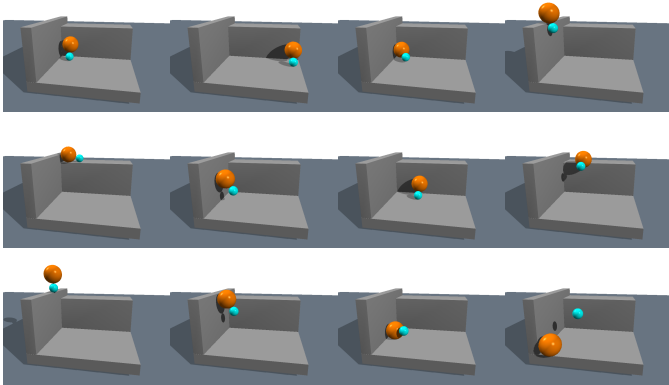


Fig. 2: Random samples from the double sphere domain.

Note that all proposed methods heavily rely on available constrained samples  $\mathcal{D}_s$ : The trajectory-based methods indirectly via  $\mathcal{D}_u$ ; the state-interpolation based methods in particular via the projection (19).

The trajectory-based approaches naturally reflect the bias that states on found trajectories are relevant to visit given a goal  $g_i$ . In relation to BC, somewhat to our surprise, this mere state initialization bias empirically turned out to be highly effective, also without BC. In this view, a core role of demonstration trajectories is demonstrating relevant “interpolating” states rather than demonstrating actions. Inspired by this view, we studied whether naive interpolation can equally be effective. However, as naive linear interpolation in generalized coordinates between two configurations is likely not feasible, we propose projected interpolation (19) using a kd-tree in  $\phi$ -space to find a nearest feasible state in  $\mathcal{D}_s$ .

Alg. 1 summarizes *Sample-Guided RL* leveraging the state and trajectory data. Lines 12-14 are standard TD7 applied to the goal-conditioned case with optional BC regularization [16, 15, 17]. Training is organized in blocks (line 10), where in each block we update the start/goal distribution depending on the phase  $\alpha$  and using options (16)-(21). As a default, we use a total of  $T_{\text{tot}} = 2M$  training steps, update start/goals every  $T_{\text{block}} = 100k$  steps, and schedule the phase to reach 1 at  $T_{\text{sched}} = 1M$ .

## V. EVALUATIONS

We evaluate how guiding RL using constrained samples and trajectory data can support training universal manipulation policies in contact-rich manipulation domains. To this end we propose novel benchmarks that are minimalistic enough to effectively study universal manipulation, but still rich in the possible manipulation strategies.

Specifically, Fig. 2 illustrates the double sphere problem, a minimalistic domain that includes a sphere object (orange), sphere robot (turquoise, 3D position controlled), and three further shapes (floor, walls) to allow

for more rich contact modes. Despite its simplicity, Fig. 2 highlights the diversity of samples under collision, contact, and force constraints (Sec. IV-A) that are feasible in this domain. We consider this an ideal test problem to study training a universal policy to reach any such random state from any other.

To test scaling to more complex domains, we also investigate a domain replacing the sphere robot by a panda arm (Fig. 1). Here, the set of  $S$  of potential support shapes includes *all* of panda’s links (made convex due to MuJoCo’s constraints) in addition to the floor and walls. Random contact modes  $c_{ij}$  include any single, double, or triplet support of the sphere by any shape. The diversity of samples we find highlight this as a domain to evaluate whole-body-contact manipulation.

We encourage viewing the accompanying video that walks through the experimental results including videos of the found behaviors.

### A. Setup

We generate  $S=10\,000$  state samples  $\mathcal{D}_s$ . As goal states where the sphere rests only on the table are trivial, we generally exclude such samples as goals.

Concerning trajectory optimization (12), we fix the total time  $T = 1\text{sec}$ , we encode  $u(t)$  as a 2nd-order B-spline with 4 knots, with the last constrained to zero velocity. A control spline is unrolled using black-box simulation stepping with 1kHz. The goal-reaching objective is implicit in the feature embedding  $\phi$  described in Sec. IV-B. We generate  $L=100\,000$  trajectories  $\mathcal{D}_u$ .

The MDP  $p(s'|s, a)$  instead steps with 20Hz. We define the agent observation as concatenation of the joint and object positions (we drop object orientation, due to invariance in our domain), joint and object velocities (including angular object velocities, scaled by 0.1), as well as the actuator state (revealing the admittance and interaction forces via the PD, scaled by 0.01) and the relative object goal. An action  $a$  is a joint position reference; more precisely, it defines a single control point B-spline in joint space starting at the current reference and ending with the zero velocity knot 0.1s in the future. This defines an arbitrary 2nd-polynomial joint position reference for the 0.05s step duration, which is unrolled with a 1kHz simulation. Actions are defined relative to the current reference position. The reward function is 1 if the object position is closer than 1cm to the goal, and zero otherwise. We chose the MDP time limit (for episode truncation) 2s for the double sphere scenario, and 4s for the panda sphere.

We left hyperparameters of TD7<sup>1</sup> [17] unchanged, except: We use  $\gamma = 0.95$  for the double sphere domain and  $\gamma = 0.99$  for the panda sphere, and reduce the exploration and target noise by half.

<sup>1</sup>We used the source code <https://github.com/sfujim/TD7>.

	double sphere	panda sphere
feasibility rate	58.7%	17.9%
evaluations per sample	30.2	105.911
time per feas. sample [msec]	17.6	350.2
total time [min]	2.93	58.4

	double sphere	panda sphere
feasibility rate	13.4%	6.87%
time per run [sec]	34.5	62.5
total time [h]	19.2	34.7

Fig. 3: Compute metrics for (a) constrained state sampling and (b) zero-order trajectory optimization.

For scheduled start/goal sampling, we use  $T_{\text{tot}} = 2M$ ,  $T_{\text{block}} = 100k$ ,  $T_{\text{sched}} = 1M$ ; for non-scheduled options we set  $T_{\text{sched}} = 1$  (implying  $\alpha = 1$ ).

#### B. Constrained State Sampling

Fig.1 illustrates random samples from our sampling method. Fig.3(a) provides compute metrics for constrained sampling. In particular, only some runs leads to feasible samples; the “time per feasible” includes the compute time spend on infeasible runs. On a laptop CPU, generating 10 000 configurations for the panda sphere domain takes about 1 hour.

#### C. Open-Loop Trajectory Optimization

We refer to the accompanying video for renderings of the found behaviors using zero-order optimization of open-loop control trajectories. The diversity of behaviors includes elaborate strategies to lift the sphere against a wall in the double sphere domain, and using all link shapes to push and scoop the sphere up its own body in the panda sphere domain. Fig. 3(b) provides compute metrics for trajectory optimization, As we employ a threshold of  $10^{-3}$ , only a few of the runs lead to feasible trajectories. We parallelized 100 000 runs in 50 processes on a CPU cluster to find 13 440 respectively 6 867 trajectories.

#### D. Sample-Guided RL

We study the effectiveness of our proposed methods to guide RL training of universal manipulation policies in our two domains. We compare six approaches:

- traj: sampling from trajectories without schedule (16)
- trajSched: same with schedule (17)
- trajSchedBC: The option of adding a BC regularization (14) to the trajSched approach.
- interp: nearest state interpolation without schedule (18)
- interpSched: same with schedule (18)
- baseline: using  $\mathcal{D}_s$  to directly draw random starts and goals without further guidance (21).

Fig. 5 provides average episode rewards (which is identical to success rate) during RL training. As detailed in the caption, average rewards depend on the current start/goal distribution during training. These training curves should therefore be discussed jointly with Fig. 6, which provides evaluations of the final policies on

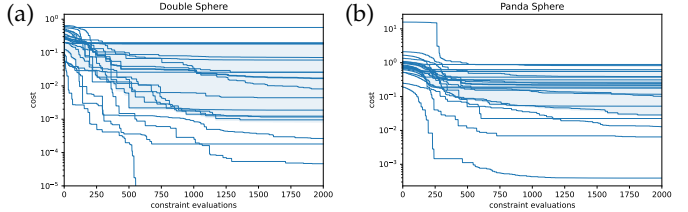


Fig. 4: Optimization runs with median (shading: 20/80% quantiles) over 20 runs, for double sphere and panda sphere domains.

the ultimate objective (3) and simplified task distributions.

Based on these evaluations, we will discuss the following:

- What is the role of BC in effective universal RL?
- How do trajectory-based methods compare to the interpolation method? Is it worth the cost of optimizing trajectories?
- How does scheduling influence performance and robustness of training?
- Where do final policies fail on the double sphere problem?

(i) BC is a dominating paradigm for transferring (model-based) demonstrations to reactive policies (see the discussion in Sec. II), and our method development was initially driven with the idea to follow this paradigm. However, our results indicate that while the state initialization method has a drastic impact on the training behavior and final performance, adding a BC objective has minor impact. Therefore, in our settings the core role of trajectories is demonstrating relevant “interpolating” states rather than demonstrating actions. This becomes more intuitive in view of the profound qualitative difference between open-loop trajectories and final policy rollouts (see the accompanying video): The policies exhibit highly reactive behavior, e.g. realizing object transports against the wall with brief reactive push maneuvers and showing recovery behavior, while the spline-based open-loop trajectories exhibit impressive strategies, but seem more conceptual rather than real-world executable. This view aligns with extensive recent work on the challenge of distilling optimization-based trajectory data into reactive policies [27, 31, 30], e.g. suggesting data augmentation to compensate for the lack of reactive control behavior in demonstrations. In our contact-rich domains, these challenges seem particularly pronounced.

(ii) Trajectories do however provide an effective method to bias state initialization: On the panda sphere problem, final policies outperform baselines and interpolation-based methods by a large factor, and training shows less variance than for other methods. On the double sphere problem, trajectory-based methods attain close to the highest performance, and are more

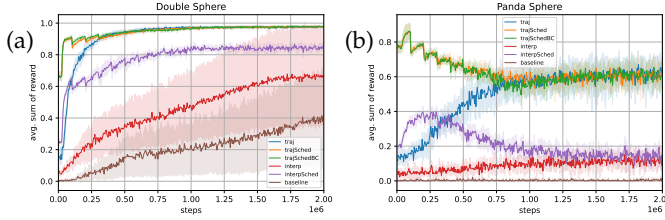


Fig. 5: Avg. episode reward (which is identical to success rate) during RL training. Mean and std. deviation (shading) over 5 independent runs for each method. Note that rewards depend on the current start/goal distribution during training, which in scheduled approaches changes every 100k steps and starts are sampled closer to goals in earlier phases – explaining *decreasing* average rewards in such methods and pronounced steps every 100k.

sample efficient than interpolation-based methods, with lower variance during training. However, the projected interpolation-based method with scheduling is surprisingly effective on the double sphere problem as well, providing the best final policy. We interpret this as an example of the classical bias-variance tradeoff: The trajectory-based methods provide a stronger prior, which pays off significantly on the harder panda sphere problem, but also implies a bias. The interpolation-based method has less bias (is closer to the ultimate  $p_0$ -objective), high variance on the panda sphere domain, but yields the (slightly) better policy on the simpler double sphere.

(iii) The previous discussion holds for the *scheduled* interpolation approach. In fact, our results indicate poor average performance, high variance, and low sample-efficiency for non-scheduled interpolation, while scheduling has less impact on trajectory-based approaches.

(iv) Finally, considering the absolute success rates in Fig. 6, in the double sphere domain we find a best success rate over random start/goals from  $\mathcal{D}_s$  (excluding trivial on-table goals) of 83.1%. Manually inspecting the failure cases, we realized that they primarily had a goal state where the sphere robot is balancing the sphere object in free space. While the sampler generates these goals (with success high rate), these configurations are unstable and beyond the control capability of our MDP and policy setup. Removing these goals, the success rate increases to 99.0%. The third column reports on the success rate on start/goal configurations on trajectories, representing the same sampling distribution as `traj`.

Concerning the panda sphere domain, we achieve a best success rate on random start/goals of 5.1% (sometimes greater than 6% for individual `traj` runs, notice the variance). While this may seem low overall, it clearly demonstrates the benefit of the proposed methods over alternatives, in particular the near-zero performance of `baseline`. Policy rollouts in the accompanying video

method	double sphere		panda shpere		
	uni	w/o balance	uni	traj	
traj	$0.801 \pm 0.008$	$0.940 \pm 0.006$	<b><math>0.981 \pm 0.002</math></b>	$0.048 \pm 0.012$	<b><math>0.612 \pm 0.073</math></b>
trajSched	$0.799 \pm 0.004$	$0.937 \pm 0.011$	<b><math>0.980 \pm 0.001</math></b>	$0.051 \pm 0.008$	<b><math>0.612 \pm 0.042</math></b>
trajSchedBC	$0.803 \pm 0.006$	$0.949 \pm 0.009$	<b><math>0.981 \pm 0.000</math></b>	$0.047 \pm 0.006$	$0.594 \pm 0.054$
interp	$0.658 \pm 0.327$	$0.787 \pm 0.389$	$0.804 \pm 0.332$	$0.020 \pm 0.004$	$0.354 \pm 0.040$
interpSched	<b><math>0.831 \pm 0.001</math></b>	<b><math>0.990 \pm 0.003</math></b>	$0.975 \pm 0.004$	$0.024 \pm 0.005$	$0.381 \pm 0.025$
baseline	$0.401 \pm 0.292$	$0.480 \pm 0.343$	$0.673 \pm 0.293$	$0.001 \pm 0.001$	$0.144 \pm 0.007$

Fig. 6: Final Policy Performance: The success rate of the final policy is evaluated over 1000 episodes. Given are mean and std. over 5 independent RL runs for each method. *uni*: evaluation of the objective (3) (with  $(s, g) \sim p_0$ ); *w/o balance*: excluding sphere-on-sphere balance goals; *traj*: evaluating only on trajectory states (consistent to `traj`).

demonstrate intricate whole-body-contact manipulation with the object. Evaluating only on start/goals from solved trajectories, the rate increases to 61.2%.

## VI. CONCLUSION

With Constrained Goal-conditioned MDPs, we proposed a novel formulation of goal-conditioned RL problems which combines standard black-box dynamics assumptions with model-based state constraints that define the start/goal distribution and provide a state visitation prior in terms of the constraint manifold. This problem formulation is a novel approach that injects first principles into RL and leverages the power of model-based constrained solvers to guide RL. Specifically, in the context of robotic manipulation, this allows us to integrate prior knowledge about collision, contact, and force constraints, exploiting our structured understanding of 3D physics, into the RL problem formulation.

We studied various approaches to guide goal-conditioned RL in this problem formulation, including BC from optimized open-loop trajectories as well as biasing and scheduling state visitation based on trajectories and constrained samples. On our proposed double sphere domain, our approaches found near perfect universal manipulation policies when excluding unstable sphere-on-sphere balancing goals. In our second domain we can demonstrate complex whole-body-contact manipulation strategies and the strong benefit of our guidance methods over the near-zero baseline.

The idea of using BC, that is to imitate the actions and thereby *dynamics* of demonstrated behavior, to guide RL is a common paradigm in current research. However, our studies indicate that *state samples* are at the core to effectively guide RL. Taking such samples from trajectories provides a strong prior and effective guidance in our domains; while adding an additional BC loss to also imitate the action distribution has minor impact. Consistent with that, our study indicated that using state samples more directly, via projected interpolation (19), can be effective (esp. in our simpler domain) and provide an alternative to trajectories.

## ACKNOWLEDGMENTS

This work has received support from the German Federal Ministry of Research, Technology and Space (BMFTR) under the Robotics Institute Germany (RIG); from the Amazon Fulfillment Technologies and Robotics team; from the French government, managed by the National Research Agency, under the France 2030 program with the references Organic Robotics Program (PEPR O2R), “PR[AI]RIE-PSAI” (ANR-23-IACL-0008) and RODEO (ANR-24-CE23-5886); and from the European Union through the ARTIFACT project (GA no.101165695) and the AGIMUS project (GA no.101070165). Views and opinions expressed are those of the author(s) only and do not necessarily reflect those of the funding agencies.

## REFERENCES

- [1] Ilge Akkaya, Marcin Andrychowicz, Maciek Chociej, Mateusz Litwin, Bob McGrew, Arthur Petron, Alex Paino, Matthias Plappert, Glenn Powell, Raphael Ribas, et al. Solving rubik’s cube with a robot hand. *arXiv:1910.07113*, 2019.
- [2] Marcin Andrychowicz, Filip Wolski, Alex Ray, Jonas Schneider, Rachel Fong, Peter Welinder, Bob McGrew, Josh Tobin, OpenAI Pieter Abbeel, and Wojciech Zaremba. Hindsight experience replay. *Advances in neural information processing systems*, 30, 2017.
- [3] Alp Aydinoglu, Adam Wei, Wei-Cheng Huang, and Michael Posa. Consensus complementarity control for multi-contact mpc. *IEEE Transactions on Robotics*, 2024.
- [4] Chenjia Bai, Peng Liu, Wei Zhao, and Xianglong Tang. Guided goal generation for hindsight multi-goal reinforcement learning. *Neurocomputing*, 359: 353–367, 2019.
- [5] Philip J Ball, Laura Smith, Ilya Kostrikov, and Sergey Levine. Efficient online reinforcement learning with offline data. In *International Conference on Machine Learning*, pages 1577–1594. PMLR, 2023.
- [6] Stephen Boyd and Lieven Vandenberghe. *Convex optimization*. Cambridge university press, 2004.
- [7] Cornelius V Braun, Sayantan Auddy, and Marc Toussaint. Trajectory first: A curriculum for discovering diverse policies. *arXiv:2506.01568*, 2025.
- [8] Andres Campero, Roberta Raileanu, Heinrich Küttler, Joshua B. Tenenbaum, Tim Rocktäschel, and Edward Grefenstette. Learning with amigo: Adversarially motivated intrinsic goals. In *9th International Conference on Learning Representations, ICLR 2021, Virtual Event, Austria, May 3-7, 2021*, 2021.
- [9] Elliot Chane-Sane, Cordelia Schmid, and Ivan Laptev. Goal-conditioned reinforcement learning with imagined subgoals. In *Proceedings of the International Conference on Machine Learning*, 2021.
- [10] Hongkai Dai, Andrés Valenzuela, and Russ Tedrake. Whole-body motion planning with centroidal dynamics and full kinematics. In *2014 IEEE-RAS International Conference on Humanoid Robots*, pages 295–302. IEEE, 2014.
- [11] Murtaza Dalal, Ajay Mandlekar, Caelan Garrett, Ankur Handa, Ruslan Salakhutdinov, and Dieter Fox. Imitating Task and Motion Planning with Visuomotor Transformers. In *Conference on Robot Learning (CoRL)*. PMLR, 2023. doi: 10.48550/arXiv.2305.16309.
- [12] Robin Deits and Russ Tedrake. Footstep planning on uneven terrain with mixed-integer convex optimization. In *2014 IEEE-RAS international conference on humanoid robots*, pages 279–286. IEEE, 2014.
- [13] Meng Fang, Tianyi Zhou, Yali Du, Lei Han, and Zhengyou Zhang. Curriculum-guided hindsight experience replay. *Advances in neural information processing systems*, 32, 2019.
- [14] Carlos Florensa, David Held, Markus Wulfmeier, Michael Zhang, and Pieter Abbeel. Reverse curriculum generation for reinforcement learning. In *Conference on Robot Learning*, pages 482–495. PMLR, 2017.
- [15] Scott Fujimoto and Shixiang Shane Gu. A minimalist approach to offline reinforcement learning. In *Advances in Neural Information Processing Systems (NeurIPS)*, volume 34, pages 20132–20145, 2021.
- [16] Scott Fujimoto, Herke Hoof, and David Meger. Addressing function approximation error in actor-critic methods. In *International Conference on Machine Learning*, pages 1587–1596. PMLR, 2018.
- [17] Scott Fujimoto, Wei-Di Chang, Edward Smith, Shixiang Shane Gu, Doina Precup, and David Meger. For sale: State-action representation learning for deep reinforcement learning. *Advances in neural information processing systems*, 36:61573–61624, 2023.
- [18] Xudong Gong, Dawei Feng, Kele Xu, Bo Ding, and Huaimin Wang. Goal-conditioned on-policy reinforcement learning. In *Advances in Neural Information Processing Systems*, 2024.
- [19] Gianluigi Grandesso, Elisa Alboni, Gastone P. Rosati Papini, Patrick M. Wensing, and Andrea Del Prete. Cacto: Continuous actor-critic with trajectory optimization—towards global optimality. *IEEE Robotics and Automation Letters*, 8(6):3318–3325, 2023.
- [20] Ruben Grandia, Espen Knoop, Michael A. Hopkins, Georg Wiedebach, Jared Bishop, Steven Pickles, David Müller, and Moritz Bächer. Design and Control of a Bipedal Robotic Character. In *Proceedings of Robotics: Science and Systems*, Delft, Netherlands, July 2024.
- [21] Abhishek Gupta, Vikash Kumar, Corey Lynch, Sergey Levine, and Karol Hausman. Relay policy learning: Solving long-horizon tasks via imitation

and reinforcement learning. In *Conference on Robot Learning*, pages 1025–1037. PMLR, 2020.

[22] Nikolaus Hansen and Andreas Ostermeier. Completely derandomized self-adaptation in evolution strategies. *Evolutionary computation*, 9(2):159–195, 2001.

[23] Lukas Hermann, Max Argus, Andreas Eitel, Artemij Amiranashvili, Wolfram Burgard, and Thomas Brox. Adaptive curriculum generation from demonstrations for sim-to-real visuomotor control. In *2020 IEEE International Conference on Robotics and Automation (ICRA)*, pages 6498–6505. IEEE, 2020.

[24] Hengyuan Hu, Suvir Mirchandani, and Dorsa Sadigh. Imitation bootstrapped reinforcement learning. In *Robotics: Science and Systems XX, Delft, The Netherlands, July 15-19, 2024*, 2024.

[25] Yuming Huang, Bin Ren, Ziming Xu, and Lianghong Wu. MRHER: model-based relay hindsight experience replay for sequential object manipulation tasks with sparse rewards. In *International Joint Conference on Neural Networks (IJCNN)*, pages 1–8. IEEE, 2024.

[26] Physical Intelligence, Ali Amin, Raichelle Aniceto, Ashwin Balakrishna, Kevin Black, Ken Conley, Grace Connors, James Darpinian, Karan Dhabalia, Jared DiCarlo, Danny Driess, Michael Equi, Adnan Esmail, Yunhao Fang, Chelsea Finn, Catherine Glossop, Thomas Godden, Ivan Goryachev, Lachy Groom, Hunter Hancock, Karol Hausman, Gashon Hussein, Brian Ichter, Szymon Jakubczak, Rowan Jen, Tim Jones, Ben Katz, Liyiming Ke, Chandra Kuchi, Marinda Lamb, Devin LeBlanc, Sergey Levine, Adrian Li-Bell, Yao Lu, Vishnu Mano, Mohith Mothukuri, Suraj Nair, Karl Pertsch, Allen Z. Ren, Charvi Sharma, Lucy Xiaoyang Shi, Laura Smith, Jost Tobias Springenberg, Kyle Stachowicz, Will Stoeckle, Alex Swerdfloor, James Tanner, Marcel Torne, Quan Vuong, Anna Walling, Haohuan Wang, Blake Williams, Sukwon Yoo, Lili Yu, Ury Zhilinsky, and Zhiyuan Zhou.  $\pi_{0.6}^*$ : a vla that learns from experience. *arXiv:2511.14759*, 2025.

[27] Mingxi Jia, Dian Wang, Guanang Su, David Klee, Xupeng Zhu, Robin Walters, and Robert Platt. SEIL: Simulation-augmented Equivariant Imitation Learning. In *IEEE International Conference on Robotics and Automation (ICRA)*, pages 1845–1851. IEEE, 2023.

[28] Mingxuan Jing, Xiaojian Ma, Wenbing Huang, Fuchun Sun, Chao Yang, Bin Fang, and Huaping Liu. Reinforcement learning from imperfect demonstrations under soft expert guidance. In *Proceedings of the AAAI conference on artificial intelligence*, volume 34, pages 5109–5116, 2020.

[29] Armand Jordana, Jianghan Zhang, Joseph Amigo, and Ludovic Righetti. An Introduction to Zero-Order Optimization Techniques for Robotics. *arXiv:2506.22087*, October 2025.

[30] Liyiming Ke, Jingqiang Wang, Tapomayukh Bhattacharjee, Byron Boots, and Siddhartha Srinivasa. Grasping with chopsticks: Combating covariate shift in model-free imitation learning for fine manipulation. In *IEEE International Conference on Robotics and Automation (ICRA)*, pages 6185–6191. IEEE, 2021.

[31] Liyiming Ke, Yunchu Zhang, Abhay Deshpande, Siddhartha Srinivasa, and Abhishek Gupta. CCIL: Continuity-based Data Augmentation for Corrective Imitation Learning. *arXiv:2310.12972*, June 2024.

[32] Florent Lamiriaux and Joseph Mirabel. Prehensile manipulation planning: Modeling, algorithms and implementation. *IEEE Transactions on Robotics*, 38(4):2370–2388, 2021.

[33] Steven M. LaValle. *Planning Algorithms*. Cambridge university press, 2006.

[34] Quentin Le Lidec, Fabian Schramm, Louis Montaut, Cordelia Schmid, Ivan Laptev, and Justin Carpentier. Leveraging randomized smoothing for optimal control of nonsmooth dynamical systems. *Nonlinear Analysis: Hybrid Systems*, 52:101468, 2024.

[35] Andrew Levy, Robert Platt, and Kate Saenko. Hierarchical actor-critic. *arXiv:1712.00948*, 2017.

[36] Erik M Lintunen, Nadia M Ady, and Christian Guckelsberger. Diversity progress for goal selection in discriminability-motivated RL. *arXiv:2411.01521*, 2024.

[37] Fukang Liu, Zhaoyuan Gu, Yilin Cai, Ziyi Zhou, Hyunyoung Jung, Jaehwi Jang, Shijie Zhao, Sehoon Ha, Yue Chen, Danfei Xu, et al. Opt2skill: Imitating dynamically-feasible whole-body trajectories for versatile humanoid loco-manipulation. *IEEE Robotics and Automation Letters*, 2025.

[38] Jinxin Liu, Donglin Wang, Qiangxing Tian, and Zhengyu Chen. Learn goal-conditioned policy with intrinsic motivation for deep reinforcement learning. In *Proceedings of the AAAI conference on artificial intelligence*, volume 36, pages 7558–7566, 2022.

[39] Tomas Lozano-Perez. A simple motion-planning algorithm for general robot manipulators. *IEEE Journal on Robotics and Automation*, 3(3):224–238, 2003.

[40] Carlos Mastalli, Rohan Budhiraja, Wolfgang Merkt, Guilhem Saurel, Bilal Hammoud, Maximilien Naveau, Justin Carpentier, Ludovic Righetti, Sethu Vijayakumar, and Nicolas Mansard. Crocodyl: An efficient and versatile framework for multi-contact optimal control. In *2020 IEEE International Conference on Robotics and Automation (ICRA)*, pages 2536–2542. IEEE, 2020.

[41] Igor Mordatch, Emanuel Todorov, and Zoran Popović. Discovery of complex behaviors through contact-invariant optimization. *ACM Transactions on Graphics (ToG)*, 31(4):1–8, 2012.

[42] Ofir Nachum, Shixiang Shane Gu, Honglak Lee, and Sergey Levine. Data-efficient hierarchical reinforcement learning. In *Advances in Neural Information Processing Systems*, 2018.

[43] Ashvin Nair, Vitchyr Pong, Murtaza Dalal, Shikhar Bahl, Steven Lin, and Sergey Levine. Visual reinforcement learning with imagined goals. In *Advances in Neural Information Processing Systems*, 2018.

[44] Ian Osband, Charles Blundell, Alexander Pritzel, and Benjamin Van Roy. Deep exploration via bootstrapped DQN. *Advances in neural information processing systems*, 29, 2016.

[45] Fabian Otto, Onur Celik, Hongyi Zhou, Hanna Ziesche, Vien Anh Ngo, and Gerhard Neumann. Deep black-box reinforcement learning with movement primitives. In *Conference on Robot Learning*, pages 1244–1265. PMLR, 2023.

[46] Sujoy Paul, Jeroen Vanbaar, and Amit Roy-Chowdhury. Learning from trajectories via subgoal discovery. *Advances in Neural Information Processing Systems*, 32, 2019.

[47] Xue Bin Peng, Pieter Abbeel, Sergey Levine, and Michiel Van de Panne. Deepmimic: Example-guided deep reinforcement learning of physics-based character skills. *ACM Transactions On Graphics (TOG)*, 37(4):1–14, 2018.

[48] Xue Bin Peng, Ze Ma, Pieter Abbeel, Sergey Levine, and Angjoo Kanazawa. Amp: Adversarial motion priors for stylized physics-based character control. *ACM Transactions on Graphics (ToG)*, 40(4):1–20, 2021.

[49] Michael Posa, Cecilia Cantu, and Russ Tedrake. A direct method for trajectory optimization of rigid bodies through contact. *The International Journal of Robotics Research*, 33(1):69–81, 2014.

[50] Tom Schaul, Daniel Horgan, Karol Gregor, and David Silver. Universal value function approximators. In *International Conference on Machine Learning*, pages 1312–1320. PMLR, 2015.

[51] Thierry Siméon, Jean-Paul Laumond, Juan Cortés, and Anis Sahbani. Manipulation planning with probabilistic roadmaps. *The International Journal of Robotics Research*, 23(7-8):729–746, 2004.

[52] Yuda Song, Yifei Zhou, Ayush Sekhari, Drew Bagwell, Akshay Krishnamurthy, and Wen Sun. Hybrid RL: Using both offline and online data can make RL efficient. In *The Eleventh International Conference on Learning Representations*, 2023.

[53] Hyung Ju Terry Suh, Tao Pang, and Russ Tedrake. Bundled gradients through contact via randomized smoothing. *IEEE Robotics and Automation Letters*, 7(2):4000–4007, 2022.

[54] Yuval Tassa, Tom Erez, and Emanuel Todorov. Synthesis and stabilization of complex behaviors through online trajectory optimization. In *2012 IEEE/RSJ International Conference on Intelligent Robots and Systems*, pages 4906–4913. IEEE, 2012.

[55] Emanuel Todorov, Tom Erez, and Yuval Tassa. Mujoco: A physics engine for model-based control. In *2012 IEEE/RSJ international conference on intelligent robots and systems*, pages 5026–5033. IEEE, 2012.

[56] Marc Toussaint, Jung-Su Ha, and Danny Driess. Describing physics for physical reasoning: Force-based sequential manipulation planning. *IEEE Robotics and Automation Letters*, 5(4):6209–6216, 2020.

[57] Alexander Trott, Stephan Zheng, Caiming Xiong, and Richard Socher. Keeping your distance: Solving sparse reward tasks using self-balancing shaped rewards. *Advances in Neural Information Processing Systems*, 32, 2019.

[58] Ikechukwu Uchendu, Ted Xiao, Yao Lu, Banghua Zhu, Mengyuan Yan, Joséphine Simon, Matthew Bennice, Chuyuan Fu, Cong Ma, Jiantao Jiao, et al. Jump-start reinforcement learning. In *International Conference on Machine Learning*, pages 34556–34583. PMLR, 2023.

[59] Núria Armengol Urpí, Marin Vlastelica, Georg Martius, and Stelian Coros. Epistemically-guided forward-backward exploration. *arxiv:2507.05477*, July 2025.

[60] Khaled Wahba, Joaquim Ortiz-Haro, Marc Toussaint, and Wolfgang Hönig. Kinodynamic motion planning for a team of multirotors transporting a cable-suspended payload in cluttered environments. In *2024 IEEE/RSJ International Conference on Intelligent Robots and Systems (IROS)*, pages 12750–12757. IEEE, 2024.

[61] Stephen Wright, Jorge Nocedal, et al. Numerical optimization. *Springer Science*, 35(67–68):7, 1999.

[62] Zhenjia Xu, Zhanpeng He, and Shuran Song. Universal manipulation policy network for articulated objects. *IEEE robotics and automation letters*, 7(2):2447–2454, 2022.